IRREVERSIBILTY AND HEAT TRANSFER STUDY IN A POROUS LID-DRIVEN CAVITY FILLED WITH A NANOFLUID USING THE DARCY-BRINKMAN FORMULATION

Souad Marzougui[1], Ammar Ben Brahim[1] and Mourad Magherbi[1,2]

Gabès University, Chemical Engineering Department,

High Institute of Applied Sciences and Technology, Omar Ibn El Khattab Street, 6029 Gabès, Tunisia

E-Mails: marzougui_souad@hotmail.fr, magherbim@yahoo.fr,

Abstract⸺**The present work reports a numerical simulation of entropy generation and heat transfer in a lid-driven porous cavity filled with a nanofluid. Given the large number of dimensionless parameters related to this problem, some of them are kept constant and therefore the other governing dimensionless number such as, the Rayleigh number, the Forchheimer parameter, the Hartman number, the Reynolds number, the volume fraction and the magnetic field inclination angle are varying in the following ranges; $10^4 \leq Ra \leq 10^6$, $0.2 \leq Fc \leq 0.9$, $10 \leq Ha \leq 50$, $20 \leq Re \leq 50$, $2\% \leq \varphi \leq 14\%$, $0° \leq \alpha \leq 180°$ Hartman number was investigated for different inclination angle of the magnetic field. Third the effect of the respectively. Firstly, the effects of the Rayleigh and Forchheimer numbers on the irreversibility are studied. Secondly, the effects of the nanoparticle volume fraction was examined for different Reynolds numbers. Results show that the flow structure is strongly affected by the increase of Ra, Re and φ. Results reveal that the irreversibility in the nanofluid can increase or decrease depending on the values of both Re and φ.**

Keywords⸺**porous media; mixed convection; entropy generation; nanoparticle**

I. Introduction

The mixed magneto-convection heat transfer in square lid driven cavities filled with a nanofluid saturated porous media has received an extensive attention in the literature according to their wide variety of engineering applications such as the cooling of electronic devices, solar collectors and energy storage, crystal growth, food processing and nuclear reactors, etc. The literature concerning convective flow in porous media is books of Bejan et al. [1], Ingham and Pop [2] and Vafai [3].

Rudraiah et al. [4] and Chamkha [5] investigated numerically the natural convection of an electrically conducting fluid in the presence of a magnetic field. Khanafer and Vafai [6] presented a numerical study of mixed-convection heat and mass transport in a lid-driven square enclosure filled with a non-Darcian fluid-saturated porous medium by using the finite volumes technique. Mixed convection in a lid-driven porous cavity in the presence of a magnetic field is studied numerically by Muthtamilselvan et al. [7] and Rahman et al. [8]. It is found that the heat transfer is strongly dependent on the strength of the magnetic field and the Darcy number. The numerical study of hydromagnetic double diffusive mixed convection in a square lid-driven cavity is performed by Dawood and Teamah [9]. They found that direction of lid is more effective on heat and mass transfer and fluid flow with increasing of magnetic field for all studied parameters. Hydrodynamic mixed convection heat transfer in a lid-driven cavity heated from top with wavy bottom surface is numerically studied by Saha et al. [10]. It is observed that the wavy lid-driven cavity can be considered as an effective heat transfer mechanism in presence of magnetic field at larger wavy surface amplitudes and low Richardson numbers. Mchirgui et al. [11] reported a numerical study of the entropy generation in double diffusive convection through a square porous cavity saturated with a binary perfect gas mixture submitted to a horizontal thermal and concentration gradients.

From our knowledge, the influence of the magnetic field, the Rayleigh and Reynolds numbers and the nanoparticle volume fraction on the irreversibility of a nanofluid in a lid-driven porous cavity have not yet been encountered. Hence, we result to study the influence of the above listed parameters on the irreversibility and heat transfer in a Darcy-Forchheimer mixed convection in nanofluid saturated lid-driven porous cavity

4ème Conférence Internationale des Energies Renouvelables (CIER-2016)
Proceedings of Engineering and Technology – PET
Vol.14, pp.101 - 110

submitted to an oriented magnetic field. The governing equations of the considered problem are solved using a licensed version of the COMSOL Multiphysics software.

II. MATHEMATICAL FORMULATION

Consider a two-dimensional laminar flow in a square lid-driven porous cavity filled with a Newtonian, incompressible nanofluid. The cavity has a height H as shown in Fig. 1.
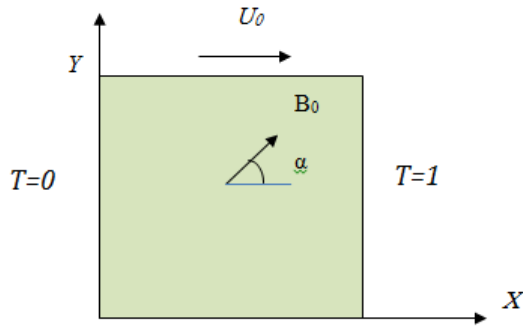

Fig.1. Schematic view of the physical model coordinate system.

The top and the bottom walls are adiabatic. The top wall is assumed to be moving from left to right at constant speed U_0. The right and the left walls are maintained at constant hot temperature (θ_h) and constant cold temperature (θ_c) respectively. A uniform magnetic field of strength B_0, making an inclination angle (α) with the horizontal, is applied in the x-y plane of the cavity. The physical properties of the fluid are considered to be constant except the density, which satisfies the Boussinesq approximation as:

$$\rho = \rho_0 \left[1 - \beta_\theta (\theta - \theta_0)\right] \qquad (1)$$

Where ρ_0 is the fluid density at temperature θ_0 and β_θ is the thermal expansion coefficient such

that: $\beta_\theta = -\dfrac{1}{\rho_0}\left(\dfrac{\partial \rho}{\partial \theta}\right)_P$

The governing equations of continuity, momentum and energy balances can be written in the dimensionless form as:
Continuity equation:

$$\frac{\partial U}{\partial X} + \frac{\partial V}{\partial Y} = 0 \qquad (2)$$

X-Momentum equation:

$$\frac{1}{\varepsilon}\frac{\partial U}{\partial \tau} + \frac{1}{\varepsilon^2}U\frac{\partial U}{\partial X} + \frac{1}{\varepsilon^2}V\frac{\partial U}{\partial Y} = \frac{\rho_f}{\rho_{nf}}\left[-\frac{\partial P}{\partial X} - \frac{\mu_{nf}}{\mu_f}\frac{1}{\varepsilon \mathrm{Re}}\nabla^2 U - \frac{\mu_{nf}}{\mu_f}\frac{U}{Da\,\mathrm{Re}}\right]$$
$$+ \frac{\rho_f}{\rho_{nf}}\frac{\sigma_{nf}}{\sigma_f}\frac{\mathrm{Ha}^2}{\mathrm{Re}}\left(V\sin\gamma\cos\gamma - U\sin^2\gamma\right) - \frac{F_c}{\sqrt{Da}}U\sqrt{U^2+V^2} \qquad (3)$$

Y-Momentum equation:

$$\frac{1}{\varepsilon}\frac{\partial V}{\partial \tau} + \frac{1}{\varepsilon^2}V\frac{\partial U}{\partial X} + \frac{1}{\varepsilon^2}V\frac{\partial V}{\partial Y} = \frac{\rho_f}{\rho_{nf}}\left[-\frac{\partial P}{\partial Y} - \frac{\mu_{nf}}{\mu_f}\frac{1}{\varepsilon \mathrm{Re}}\nabla^2 V - \frac{\mu_{nf}}{\mu_f}\frac{V}{Da\,\mathrm{Re}} + \frac{(\rho\beta)_{nf}}{(\rho\beta)_f}Ri\,\theta\right]$$
$$+ \frac{\rho_f}{\rho_{nf}}\frac{\sigma_{nf}}{\sigma_f}\frac{\mathrm{Ha}^2}{\mathrm{Re}}\left(U\sin\gamma\cos\gamma - V\cos^2\gamma\right) - \frac{F_c}{\sqrt{Da}}V\sqrt{U^2+V^2}$$
$$(4)$$

Energy equation:

$$\frac{\partial T}{\partial \tau} + U\frac{\partial T}{\partial X} + V\frac{\partial T}{\partial Y} = \frac{\alpha_{nf}}{\alpha_f}\frac{1}{\mathrm{Pr\,Re}}\left(\frac{\partial^2 T}{\partial^2 X} + \frac{\partial^2 T}{\partial^2 Y}\right) \qquad (5)$$

Where the dimensionless parameters are defined in the following forms,

$$X = \frac{x}{H};\ Y = \frac{y}{H};\ \mathrm{U} = \frac{u}{U_0};\ V = \frac{v}{U_0};$$

$$P = \frac{p}{\rho_f U_0^2};\ \tau = \frac{U_0 t}{H};\ T = \frac{\theta - \theta_c}{\theta_h - \theta_c};\ \mathrm{Pr} = \frac{v_f}{\alpha_f};$$

$$\mathrm{Re} = \frac{U_0 H}{v_f};\ Da = \frac{K}{H^2};\ Ha = B_0 H\sqrt{\frac{\sigma_f}{\mu_f}};$$

$$Ri = \frac{Ra}{Pe\,\mathrm{Re}};\ Ra = \frac{g\beta_\theta(\theta_h - \theta_c)L^3}{v_f\,\alpha_f};$$

$$F_c = \left(1.75\big/\sqrt{150\varepsilon^2}\right);\ Pe = Re\,Pr$$

The parameters F_C, Ha, Ri, Pe and Pr are respectively Forchheimer, Hartman, Richardson, Peclet and Prandtl numbers.

The expressions of density, thermal expansion, heat capacitance, dynamic viscosity, electrical conductivity, thermal conductivity and thermal diffusivity of the nanofluid are given as follows [12]:

$$\rho_{nf} = (1-\varphi)\rho_f + \varphi\rho_s \qquad (6)$$

$$(\rho\beta)_{nf} = (1-\varphi)(\rho\beta)_f + \varphi(\rho\beta)_s \qquad (7)$$

$$(\rho c_p)_{nf} = (1-\varphi)(\rho c_p)_f + \varphi(\rho c_p)_s \qquad (8)$$

$$\frac{\mu_{nf}}{\mu_f} = \frac{1}{(1-\varphi)^{2,5}} \qquad (9)$$

$$\frac{\sigma_{eff}}{\sigma_f} = 1 + \frac{3(\alpha-1)\varphi}{(2+\alpha)-(\alpha-1)\varphi};\ \alpha = \frac{\sigma_s}{\sigma_f} \qquad (10)$$

$$\frac{k_{nf}}{k_f} = \frac{k_s + 2k_f - 2\varphi(k_f - k_s)}{k_s + 2k_f + \varphi(k_f - k_s)} \qquad (11)$$

$$\alpha_{nf} = \frac{k_{nf}}{(\rho c_p)_{nf}} \qquad (12)$$

2

4ème Conférence Internationale des Energies Renouvelables (CIER-2016)
Proceedings of Engineering and Technology – PET
Vol.14, pp.101 - 110

The initial and boundary conditions, expressed in dimensionless form are:

Initial conditions

$U(X,Y) = 0$ $\begin{array}{c} V(X,Y) = P \\ = 0 \end{array}$ $T(X,Y) = 0$ (13-a)

Vertical adiabatic walls

$U(1,Y) = 0$ $V(1,Y) = 0$ $T(1,Y) = 1$ (13-b)

$U(0,Y) = 0$ $V(0,Y) = 0$ $T(0,y) = 0$ (13-c)

Horizontal active walls

$U(1,y) = 1$ $V(1,y) = 0$ $\dfrac{\partial T}{\partial X} = 0$ (13-d)

$U(0,Y) = 0$ $V(0,y) = 0$ $\dfrac{\partial T}{\partial X} = 0$ (13-e)

The Nusselt number, is defined as follow:

$$\mathrm{N}u = -\frac{k_{nf}}{k_f}\int_0^1 (\frac{\partial T}{\partial Y})dX \quad (14)$$

III. SECOND LAW FORMULATION

The local entropy generation in porous media is given by Woods (1975). In the right hand side of Eq. (14), the first term of is the irreversibility due to heat transfer, the second represents the Darcy viscous dissipation term, the third is compatible to the clear fluid friction and the fourth is relative to the magnetic effect.

$$S_l = \left(\frac{k_{nf}}{k_f}\right)\left[\left(\frac{\partial T}{\partial X}\right)^2 + \left(\frac{\partial T}{\partial Y}\right)^2\right] + \frac{\mu_{nf}}{\mu_f}\frac{Br^*}{Da}(U^2 + V^2)$$

$$+ \left(\frac{\mu_{nf}}{\mu_f}\right)Br^*\left(2\left(\frac{\partial U}{\partial X}\right)^2 + 2\left(\frac{\partial V}{\partial Y}\right)^2 + \left(\frac{\partial U}{\partial Y} + \frac{\partial V}{\partial X}\right)^2\right) + Br^* Ha^2\left(\frac{\sigma_{nf}}{\sigma_f}\right)(Usin(\alpha) + Vcos(\alpha))^2$$

(15)

The modified Brinkman number Br^* is expressed as:

$$Br^* = \frac{\mu_f \theta_0}{k_f}\left(\frac{U_0}{\theta_h - \theta_c}\right)^2 \quad (16)$$

The dimensionless total entropy generation is given by:

$$S = \int_W S_l \, dW \quad (17)$$

IV. NUMERICAL METHOD AND TEST ACCURACY

We solve the model of Navier Stokes for an incompressible Newtonian fluid, consisting on the equations of conservation of momentum (Eq.3-4)and energy(Eq.5), with the appropriate boundary conditions (Eq.13-a,13-b, 13-c, 13-d and 13-e). COMSOL Multiphysics bases the discretization of the equations on the finite element method. The stabilization of the numerical procedure is assured by the streamline diffusion method. These governing equations are solved by a time dependent parallel sparse direct solver (PARDISO) with nested dissection multithreaded preordering algorithm. No slip boundary condition is used on the walls of the cavity.

From the known temperature and velocity fields at any time and any node of the physical model, by solving equation (3-4-5), the partial derivates of the velocity components and the temperature are calculated in the variables attribute node of the COMSOL program model builder. Simultaneously, the local entropy generation related to the thermal gradient, the viscous fluid friction, and the Darcy viscous fluid are evaluated at any time (t), and any nodal point of the physical system. Thereafter, the total entropy generation related to each cause of irreversibility is calculated. The total entropy generation of all causes of irreversibility is then also calculated.

Since the entropy generation is a function of thermal and velocity gradients, it can be a good criterion for grid dependence analysis. For this reason it was used the average value of the entropy generation at the steady state. Results show that, when we pass from grid G1with 1014 elements to the grid G2 with 2518 elements the average entropy generation takes an increase of 1.2%. When we pass from the grid G2 to the grid G3 with 6614 elements the average entropy generation increases of about 0.23%.Thus, we conclude that the grid G2 with 2518 elements, is sufficient to carry out the numerical study. In this context, the grid G2 is composed of 288 quadrilateral elements near the active walls of the channel and 2230 triangular elements distributed on the remaining area.

For accuracy test, numerical results given by COMSOL's program are compared with other numerical results given by our numerical code developed in our Research Laboratory of Applied Thermodynamics. This numerical code, written in FORTRAN language, consists on a modified version of Control volume Finite-Elements (CVFEM) of Sabaas and Baliga [13] adapted to standard staggered grid at different points. The SIMPLER algorithm was applied to resolve the pressure-velocity coupling in conjunction with an Alternating Direction Implicit (ADI) scheme for

4ème Conférence Internationale des Energies Renouvelables (CIER-2016)
Proceedings of Engineering and Technology – PET
Vol.14, pp.101 - 110

performing the time evolution. This FORTRAN code, used to confirm the accuracy of numerical results given by the COMSOl's program, is validated in details in Abbassi et al. [14-15]. The validation test concerns the irreversibility maps at steady state and the entropy generation fluctuation at the onset of natural convection at different Rayleigh numbers.

As can be seen from figures 2 and 3, results given by our laboratory code and our COMSOL code are generally in good agreement. The thermal irreversibility maps given by the two codes are nearly identical. Also the pseudo-periodic fluctuation of the total entropy generation seen in the transient state of natural convection, at $Ra=10^5$ and 10^4 (Magherbi et al. [16]) given by our laboratory code are confirmed by our COMSOL code. The asymptotic behavior of the total entropy generation at $Ra=10^3$, which proves that the system is in the linear branch of the thermodynamics of irreversible processes, is also seen by the COMSOL code.

V. RESULTS AND DISCUSSION

The present study is reported to investigate the entropy generation due to mixed magneto-convection in a lid-driven square cavity filled with Darcy–Brinkman-Forchheimer saturated porous medium. The configuration considered in this work is filled by a fluid with Pr=7. The study conducted several numerical results for different dimensionless parameters that control the physics of the problem.

5.1. Effect of the Rayleigh number

The Darcy, Reynolds, Hartman and Prandtl numbers are fixed at 0.001, 20, 10 and 7. The Inclination angle of the magnetic field is zero. The nanoparticle concentration is equal to 0.05.

Fig. 2a shows one cell which occupies the entire of the cavity at $Ra=10^4$. This is due to the fact that buoyancy force are insignificant related to the inertial force which imposes the flow structure. At $Ra=5.10^4$, the cell described above becomes confined in the top part of the porous driven-cavity because of the birth of a second cell in the bottom part of the cavity. In fact in this case the increase of Ra induces an enhancement of the convection which wills in turn increases the buoyancy force. This later becomes dominant in the bottom part of the porous cavity. As Ra increases the top cell is more confined at the top wall, whereas the bottom cell elongates and occupies almost the entire cavity, which implies a dominance of the buoyancy force practically in the entire driven cavity. It's important to note that the top cell due to the advection inertial

force turns in the clockwise direction, whereas the bottom cell turns in the anti-clockwise direction. At relatively small Ra, Fig.2b indicates that the isotherms are nearly parallel to the active walls in the bottom half of the porous cavity. In this case, a conduction regime occurs in this part of the cavity. A distortion of the isotherms was seen in the top of the cavity due to the advection phenomenon. As Ra increases, the distortion of the isotherms become more pronounced even in the bottom of the cavity due to the enhancement of the convection as explain before. The total entropy generation is plotted in Fig.3, for Rayleigh number and Forchheimer parameter in the ranges respectively of $10^4 \le Ra \le 10^6$ and $0.2 \le Fc \le 0.9$.
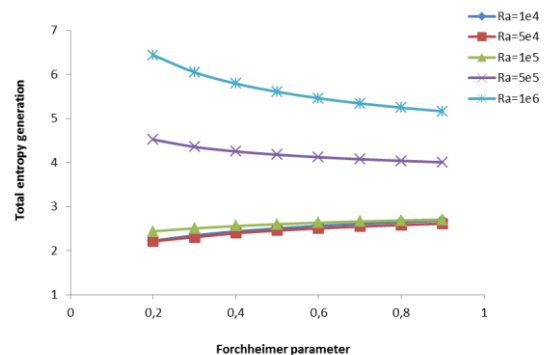

Fig.5 Total entropy evolution with the forchheimer parameter for different Rayleigh number

It's clear that only the heat transfer irreversibility persists. The other causes of irreversibility are insignificants due to the chosen values of the Darcy and Brinkman numbers. As can be seen from Fig.5, the total entropy generation slightly increases with the Forchheimer parameter for Ra smaller than critical Rayleigh number $Ra_c=2.10^5$. Additionally, at fixed Forchheimer parameter the increase of the total entropy generation with Ra is also negligible. From Ra_c the total entropy takes relatively important values at small Forchheimer parameter and then it decreases when the Forchheimer parameter increases. This behaviour of the total entropy generation can be explained by the plot in Fig.4 of the average Nusselt number at the heated wall.
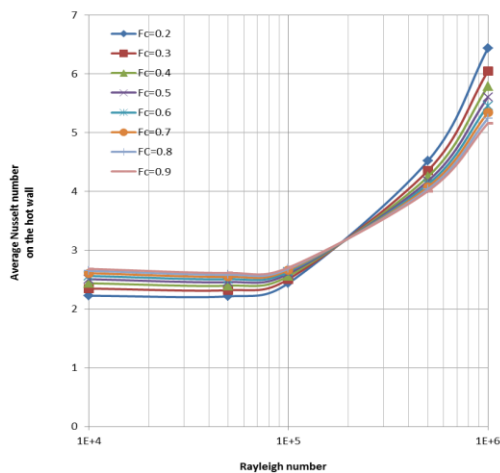
4

4$^{\text{ème}}$ Conférence Internationale des Energies Renouvelables (CIER-2016)
Proceedings of Engineering and Technology – PET
Vol.14, pp.101 - 110

Figure 6: Total entropy generation versus Rayleigh number
(Re=20, fi=0.05, alfa=0, Ha=20)

Fig.5 Total entropy generation versus Rayleigh number

(Re=20, fi=0.05, alfa=0, Ha=20)

Fig6 shows that average Nusselt generally increases with Ra for all Forchheimer parameters and this increase is most important for Ra greater than Rac. The important result from this figure is that for a fixed Ra<Rac, the heat transfer between the hot wall and the fluid increases with the Forchheimer parameter, whereas at fixed Ra>Rac the heat transfer increases when decreasing the Forchheimer parameter. This change on the Nusselt number behaviour before and after the critical Rayleigh number (Rac) can be the result of the Forchheimer parameter effect on the flow structure. Results reveal that, the increase of the Forchheimer parameter induces an elongation of the vortex due to the advection phenomena. At small Ra, the elongation of this unique vortex leads to an enhancement of the heat transfer between the hot wall and the fluid and consequently to an increase of the Nusselt number. In this case, one can observe important thermal gradients in the upper corner of the cavity and therefore important heat transfer irreversibility in this region. At high Ra fluid flow, which is characterized by a double vortex structure, the heat transfer is dominated by the convective cell which exhibits an elongation along the diagonal between the low and the upper corners of the hot and the cold walls respectively and which occupies practically the entire cavity. The resulting elongation of the upper vortex due to the increase of the Forchheimer parameter leads to a reduction of the convective vortex and consequently a decrease in the heat transfer. This decrease causes attenuation in the thermal gradients and in turn a diminution in the thermal entropy generation and therefore in the total entropy generation. This latter is principally localised in the lower and upper the hot wall and in the upper corner of the cold wall.

5

It's important to note that for Rac the Forchheimer parameter is without effect on the Nusselt number.

5.2. Effects of the Hartmann number and the magnetic field inclination angle

The Darcy, Reynolds, Rayleigh and Prandtl numbers are fixed at 0.001, 20, 10^6 and 7. The nanoparticle concentration is equal to 0.05 and the Forchheimer number is fixed to 0.404. The Hartman number and the inclination angle of the magnetic field are ranging from 0 to 50 and from 0° to 180°. The magnetic field has no intrinsic effect on the entropy generation, since the magnetic irreversibility remains negligible due to the small chosen value of the Brinkman number. But it has extrinsic effect through the momentum balance because it can affect the velocity vector which in turn induces a change in the flow structure. As seen in Fig.5, the total entropy generation exhibits an oscillatory behaviour, when the inclination angle varies from 0° to 180°.
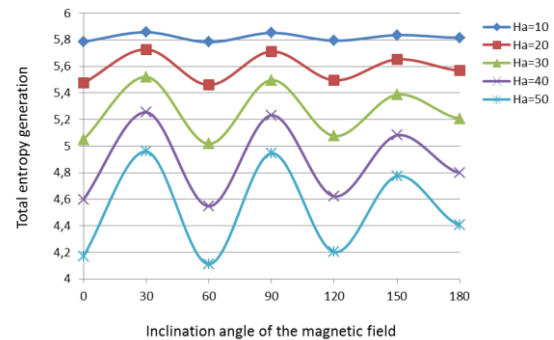

Figure 7: Effect of the magnetic field inclination angle on the entropy generation

Fig .7 : Effect of the magnetic field inclination angle on the entropy generation

In general case, total entropy generation is minimum at 60° and maximum at 30°. This can be the result of a change in the flow structure as seen in Fig.8, which illustrates the stream function and the isotherms in the lid-driven cavity at magnetic field inclination angle 0°, 30° and 90°. It's clear that the heat transfer is performed by the couple of advection-convection vortices. Figure 8 shows that, when the inclination angle increases from 0° to 30°, the top vortex becomes confined practically in the upper right corner of the cavity.

In return, the convective vortex elongates with the formation of two eggs shaped centres and also the development of two viscous boundaries layers, which leads to an enhancement of the heat transfer and consequently an increase in the entropy generation via essentially the thermal irreversibility. The structure of the flow at magnetic field inclination angle 60° looks like the structure related to the inclination angle 0°, which gives approximatively the same values of the entropy generation for the two cited angles. It's important

4$^{\text{ème}}$ Conférence Internationale des Energies Renouvelables (CIER-2016)
Proceedings of Engineering and Technology – PET
Vol.14, pp.101 - 110

to notice that the average value of the total entropy generation decrease when the Hartman number increases and one can see a decrease from 5.8 to 4.55 when Ha passes from 10 to 50. This can be explained by the slowdown character applied by the magnetic field on the fluid flow.

5.3. Effects of the Hartmann number and the nanoparticle volume fraction

The Darcy, Rayleigh and Prandtl numbers are fixed at 0.001, 10^5 and 7 respectively. The magnetic field is zero and the Forchheimer number is fixed to 0.404. The nanoparticle concentration is varying from 0 to 14% and the Reynolds number is changing from 20 to 50. There is no magnetic irreversibility since the magnetic field is zero, also the Darcy and clear fluid viscous irreversibilities are insignificants because of the chosen values of Darcy and modified Brinkman numbers. Fig.9 shows that, for Re is smaller than 30, the total entropy generation decreases when the nanoparticle volume fraction increases and reaches a constant value when the nanoparticle fraction tends towards 20%. For Re greater than 30 two opposite effects of the nanoparticle volume fraction on the total irreversibility are seen. The first corresponds to a decrease of the entropy generation when the nanoparticle fraction increases from 0 to 8% (Fig.9).
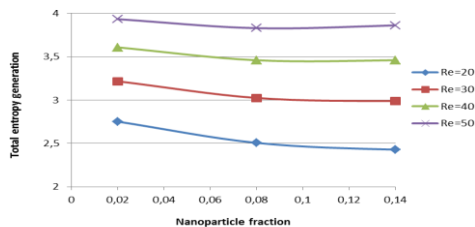

Figure 9: Nanoparticle fraction effect on entropy generation for different Re

Fig.9 Nanoparticle fraction effect on entropy generation for differnt Re

The second concerns the increase of the entropy generation when the nanoparticle fraction passes from 8% to 20%. The average Nusselt number variation (Nu) at the hot wall, which is plotted in Fig.10, looks like to the entropy generation one. This is obvious since the thermal irreversibility is the dominant cause in the total entropy generation. One can see from Fig.10 that for Reynolds number smaller than 30, the Nusselt number decreases until the nanoparticle volume fraction reaches 8%, after which it increases till the nanoparticle volume fraction achieves 14%. The thermal energy received by the fluid is the accumulation of two parts exchanged between the hot wall from one hand and the two vortices from the other, which their structures are strongly affected by nanoparticles addition.
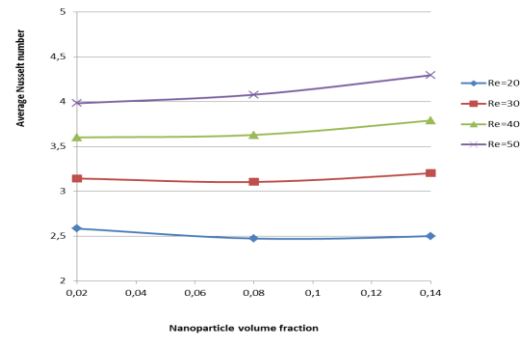
Figure 10: Nanoparticle volume fraction effect on average Nusselt number

Fig. 10 Nanoparticle volume fraction effect on Average Nusselt number

Results show that, when the nanoparticle volume fraction increases, the upper vortex elongates and leads to an increase and a decrease in the heat transfer exchanged with the hot wall. Whereas the bottom vortex reduces and induces a decrease in the heat transfer exchanged with the hot wall. In the range between 0% and 8% on the volume fraction nanoparticle, the decrease in the heat transfer between the bottom vortex and the fluid is dominant and leads consequently to a diminution in the average Nusselt number. Whereas when the nanoparticle volume fraction exceeds 8%, the enhancement of heat transfer between the hot wall and the upper vortex becomes dominant and induces an augmentation of the average Nusselt number. At relatively high Re and for small nanoparticle concentration the Nusselt number remains constant. This may be due to the fact that, the diminution of heat transfer by the bottom cell corresponds practically to the increase of heat transfer by the upper cell. When the nanoparticle concentration increases, the upper vortex is well developed which engenders an increase in the heat transfer and the Nusselt number.

V. Conclusion

In this study, we have investigate the effects of the Rayleigh number, the Hartman number, the Reynolds number, the magnetic field inclination angle and the nanoparticle volume fraction on the irreversibility and heat transfer in Darcy-Forchheimer nanofluid saturated lid-driven porous medium. The main observations are as follows:

- The total entropy generation slightly increases with the Forchheimer parameter for Ra smaller than critical Rayleigh number Rac=2.10^5.

- From Rac the total entropy takes relatively important values at small Forchheimer parameter and then it decreases when the Forchheimer parameter increases.

- At fixed Ra<Rac, the heat transfer between the hot wall and the fluid increases with the Forchheimer parameter, whereas at fixed Ra>Rac the heat transfer increases when the Forchheimer parameter

decreases. For Ra=Rac the Forchheimer parameter is without effect on the Nusselt number.

- The total entropy generation oscillates when the inclination angle varies from 0° to 180° and takes minimum value at 60° and maximum value at 30°.

- The average value of the total entropy generation decreases when the Hartman number increases.

- For Re smaller than 30, the total entropy generation decreases when the nanoparticle fraction increases and reaches a constant value when the nanoparticle fraction tends towards 14%.
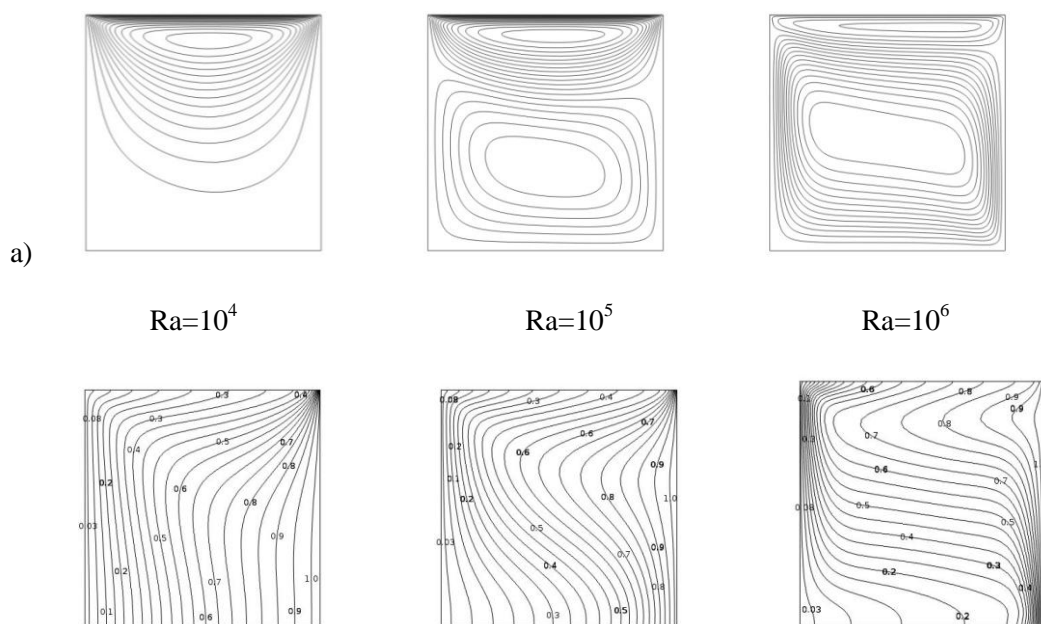
- For Re greater then 30, the entropy generation decrease when the nanoparticle fraction increases from 0 to 8% and increases when the nanoparticle volume fraction passes from 8% to 14%.

- At relatively high Re the Nusselt number increases with the nanoparticle volume fraction. The increase is more significant when the nanoparticle is greater than 8%

References

[1]   [1] D.A., Nield and A., Bejan, Convection in Porous Media, third ed., Springer, New York, (2006),

[2]   [2] D.B., Ingham and I., Pop (Eds.), Transport Phenomena in Porous Media, Elsevier, Oxford, (2005),

[3]   [3] K., Vafai (Ed.), Handbook of Porous Media, second ed., Taylor & Francis, Boca Raton, FL, (2005),

[4]   [4]N., Rudraiah, R.M., Barron, M., Venkatachalappa, and C.K., Subbaraya, Effect of a magnetic field on free convection in a rectangular enclosure, Int. J. Eng. Sci. (33), 1075-1084 (1995),

[5]   [5] A.J., Chamkha, Hydromagnetic combined convection flow in a vertical lid- driven cavity with internal heat generation or absorption, Numerical Heat Transfer Part A-Application (41), 529-546 (2002),

[6]   [6] K., Khanafer and K., Vafai, Double-diffusive mixed convection in a lid-driven enclosure filled with a fluid saturated porous medium, Numerical Heat Transfer, Part A (42), 465-486 (2002),

[7]   [7] M., Muthtamilselvan, P., Kandaswamy, and J., Lee, Hydromagnetic mixed convection in a lid-driven cavity filled with a fluid-saturated porous medium, Int. J. of Appl. Math. and Mech. 5(7), 28-44 (2009),

[8]   [8] M.M., Rahman, M.M., Billah, M.A.H., Mamun, R., Saidur and M., Hasanuzzaman, Reynolds and Prandtl numbers effects on MHD mixed convection in a lid-driven cavity along with joule heating and a centred heat conducting circular block, Int. J. of Mech. and Mat. Eng. (IJMME) (5), 163-170 (2010),

[9]   [9] M.M.K., Dawood and M.A., Teamah, Hydro-Magnetic Mixed convection double diffusive in a lid driven square cavity, European Journal of Scientific Research 85 (3), 336-355 (2012),

[10]   [10] L.K., Saha, M.C., Somadder and N.C., Roy, Hydro-magnetic mixed convection flow in a lid-driven cavity with wavy bottom surface, American Journal of Applied Mathematics 3(1-1), 8-19 (2015),

[11]   [11] A. Mchirgui, N. Hidouri, M. Magherbi and A.B. Brahim, Entropy Generation in Double-Diffusive Convection in a Square Porous Cavity using Darcy–Brinkman Formulation, Transport in Porous Media , 86 (2), 1-20, 2012.

[12]   [12] O.Mahian, A.Kianifar, C. Kleinstreuer, M. A. Al-Nimr, I. Pop, S. Wongwises, A.Z. Sahin, A review of entropy generation in nanofluid flow, International journal of Mass and Heat Transfer, Volume 65, 514-532.

[13]   [13]H.J., Saabas and B.R., Baliga, Co-located equal-order control volume finite element method for multidimensional incompressible fluid flow, Part I: FNHT Pt. B-Fund (26), 381–407(1994),

[14]   [14]H., Abbassi, S., Turki and S., Ben Nasrallah, Mixed convection in a plane channel with a built-in triangular prism, HTPA (39), 307–320 (2001),

[15]   [15] H. Abbassi,.S,Turki and S., Ben Nasrallah, Numerical investigation of forced convection in a plane channel with a built-in triangular prism, IJTS (40), 649–658 (2001),

[16]   [16] M. Magherbi, H. Abbassi and A. Ben Brahim. Entropy generation at the onset of natural convection. International Journal of Heat and Mass Transfer 46, 3441-3450, (2003)

a)   Ra=10^4 Ra=10^5 Ra=10^6

4ème Conférence Internationale des Energies Renouvelables (CIER-2016)
Proceedings of Engineering and Technology – PET
Vol.14, pp.101 - 110

b)

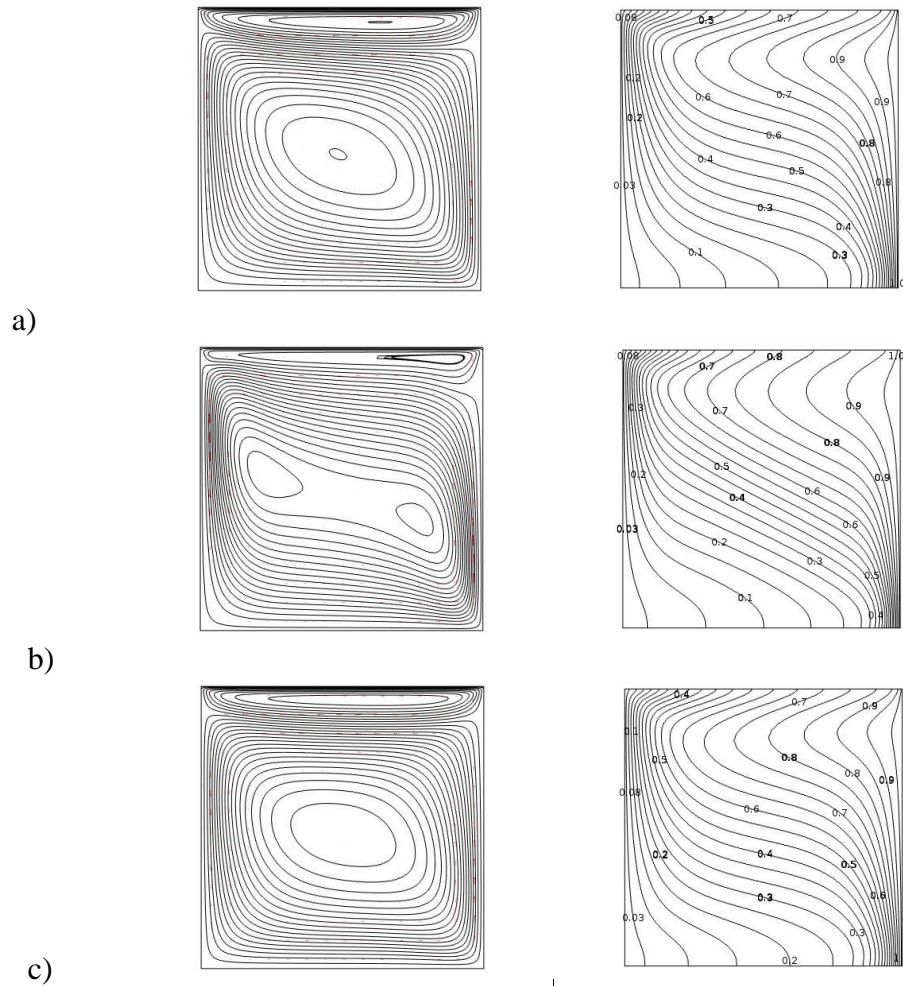Figure 2: Rayleigh number effect on: a) stream function, b) isotherms

a)

b)

c)

Figure 6: Stream function of the flow in the Lid-driven cavity at a) 0°, b) 30° and c) 90°

Table1: Physical properties of water and Cu

	ρ (Kg.m^{-3})	Cp (J.Kg^{-1}.K^{-1})	K (W.m^{-1}.K^{-1})	B (k^{-1})
water	997.1	4179	0.613	$2.1*10^{-4}$
Cu	8933	385	400	$1.67*10^{-5}$

8

9